

# THE LATE 1960S GLOBAL CLIMATE SHIFT AND ITS INFLUENCE ON THE SOUTHERN HEMISPHERE

Peter G. Baines\*

Dept. of Civil and Environmental Engineering  
University of Melbourne, Melbourne 3010, Australia

## 1. INTRODUCTION

A substantial global climate shift occurred in the late 1960s. This event did not affect everything everywhere, but it had substantial impact in certain areas, was dynamically coordinated, and was global in scale. It was manifested in changes in the sea surface temperature (SST) and tropical rainfall, with consequent changes in the atmospheric circulation of the upper and lower troposphere. These changes were largest in the season June-July-August (JJA), with smaller changes occurring in other seasons. Here the main properties of this climate shift and the regions most affected are briefly described, together with associated dynamical mechanisms, focusing on the season JJA. Data employed include SST data sets from the Hadley Centre, rainfall data from the University of East Anglia, and the re-analysis data sets from NCEP/NCAR and ERA40 from ECMWF. Figure 1 shows the low frequency temporal variability of some variables. Note that the well-known decrease in the Sahel rainfall is part of this global change. Aspects of this change as they affect Southwest Western Australia are described in Baines (2005 – pdf available via web site), and a more detailed description will be forthcoming in Baines & Folland (2006 – submitted to J. Climate).

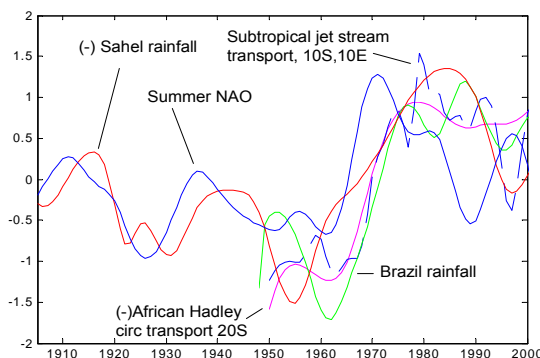


**Figure 1.** Low frequency variability of some of the principal variables that show the late 1960s climate shift for June-August (interannual variability has been removed). Details: Sahel rainfall (red): Hadley Centre data, 10°-20°N, 10°W-25°E; Brazilian rainfall (green): NCEP data, 10°S to 10°N, 90°W to 40°W; 60°W to 60°E, NCEP data; Southern node of Summer NAO in July and August (blue), Hadley Centre data; African Hadley circulation transport at 20°S (magenta), 20°W – 20°E, NCEP data; Southern subtropical jet stream transport at 10E (blue-dashed), NCEP data.

Corresponding author address: Peter G. Baines,  
Dept. of Civil and Environmental Engineering,  
University of Melbourne, Melbourne VIC 3010,  
Australia; email: [p.baines@unimelb.edu.au](mailto:p.baines@unimelb.edu.au),  
<http://www.civenv.unimelb.edu.au/~baines/>

## 2. SEA SURFACE TEMPERATURE

Changes in SST may be conveniently described by EOFs. Figure 2 shows the spatial pattern of the fourth EOF from the MOHSST data set for the annual mean SST. For this data set, the first mode shows a global warming pattern, and the second and third show El-Niño related patterns. This fourth mode shows a pattern of cooling in the North Atlantic with

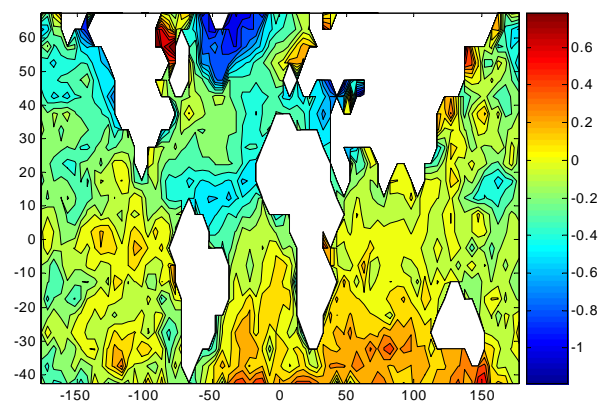


**Figure 2a.** The spatial structure for the fourth EOF for annual mean sea surface temperature – the interhemispheric mode, obtained from the MOHSST data set over the latitude range 45S to 70N, from 1911 - 2004. This EOF contains 3.6% of the total variance over this period, and 7.6% of the variance in the first 10 EOFs.

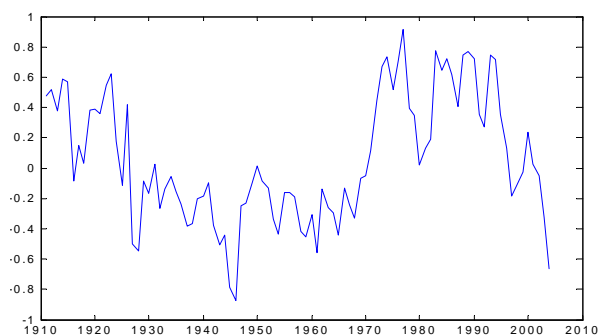


**Figure 2b.** Amplitude of the fourth EOF from 1911-2004 shown in Figure 3a. Units are degrees C.

warming in the South Atlantic and Indian Ocean. An abrupt positive increase in this pattern is evident in the late 1960s, though other changes are evident in the 1920s and 1990s.

### 3. TROPICAL RAINFALL

Tropical rainfall is a very important variable here because it gives a measure of the latent heat released that drives most of the atmospheric circulation (e.g. Peixoto & Oort 1992). For the remainder of this paper, we concentrate on the season June-August (JJA). Figure 3 shows the mean rainfall for JJA from the NCEP reanalysis (Kalnay et al. 1996, Kister et al. 2001) for the period 1958-1967. This represents the mean rainfall prior to the 1960s shift.

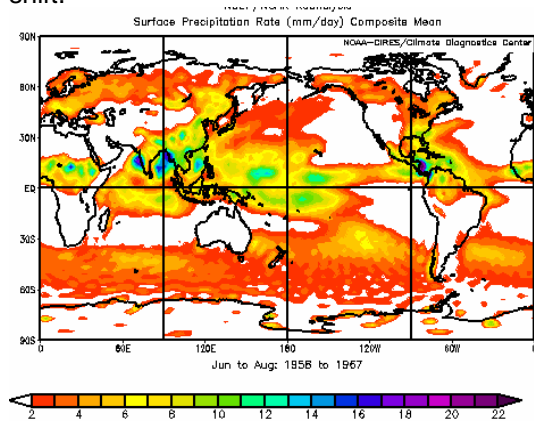


**Figure 3.** Mean rainfall for the 10-year period 1958-1967 for the season June-August, from NCEP/NCAR reanalysis. Units: mm/day.

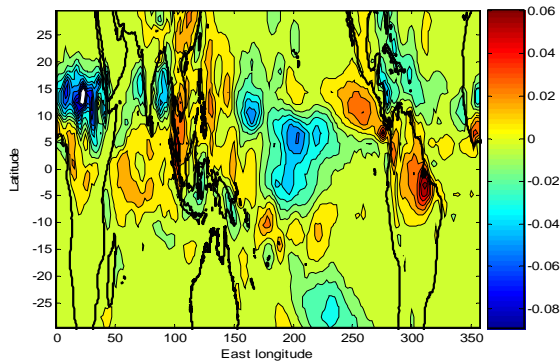


**Figure 4a.** The spatial structure of the first empirical orthogonal function for tropical rainfall anomalies (30S to 30N) based on the covariance matrix for June-August, for JJA for the period 1948-2004, obtained using NCEP/NCAR reanalysis data. Zero is a contour, with interval 0.1.

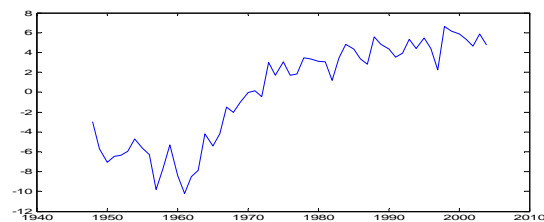


**Figure 4b.** Unfiltered amplitude of the rainfall EOF shown in Figure 4a, 1948-2004, units: mm/day.

Figure 4 shows the first EOF for JJA tropical rainfall from the NCEP reanalysis data set, for the period 1948-2004, which contains 27.5% of the total variance. Here there is a substantial change in amplitude over the late 1960s, with the principal features being a decrease in rainfall in North Africa that may be identified with the onset of the Sahel drought, an increase in South America, and a decrease in the central Pacific.

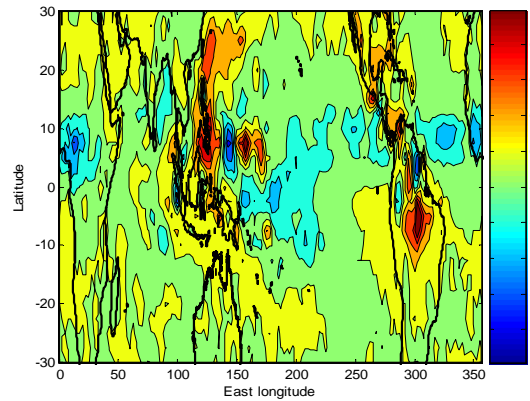


**Figure 5a** Spatial structure of the third EOF for the ECMWF ERA40 data set for JJA over the period 1958-2002. Compare with Fig. 4.

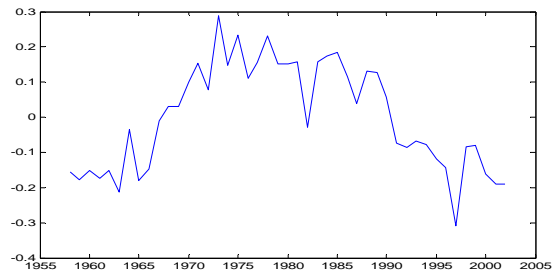


**Figure 5b.** Unfiltered amplitude of the third EOF for ECMWF rainfall shown in Figure 5a.

The corresponding mode from the ECMWF ERA40 data set is shown in Figure 5 for comparison. Here the same pattern appears in EOF 3, with 8.1% of total variance, where EOF 1 resembles global warming and EOF 2, El Niño. Hence, despite their differences, this pattern of rainfall change across the late 1960s is quite evident in both reanalyses, though the records differ in recent years. A similar EOF for raingauge data with corresponding temporal variation has been found by Lau and Sheu (1990).

### 4. CHANGES IN ATMOSPHERIC CIRCULATION.

Figure 6 shows the broad scale changes across the late 1960s in the upper troposphere, represented by flow at the 200 hPa level.

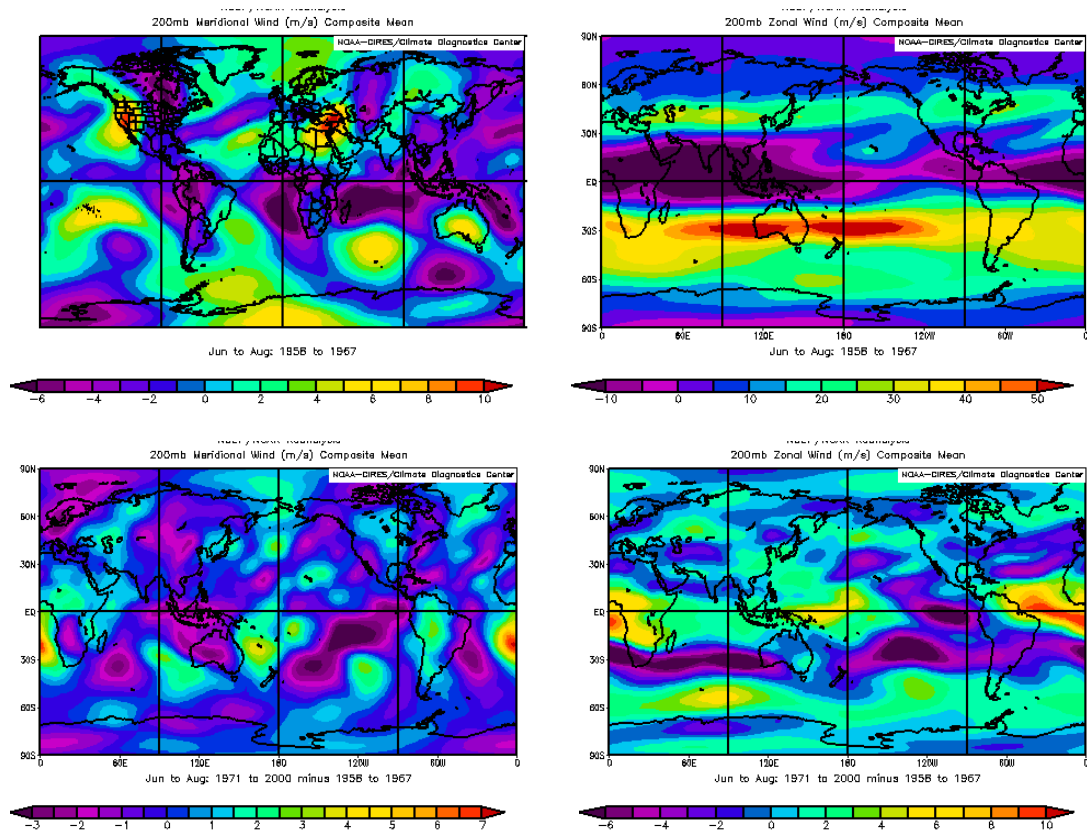


**Figure 6.** Changes in circulation at 200 hPa for JJA across the late 1960s according to the NCEP reanalysis. Panels on the left denote meridional V-component of wind, on the right, zonal U-component of wind. Upper panels denote the mean state for 1958-1967, the lower two panels the difference between the mean for 1971-2000 and 1958-1967.

A significant decrease is noted in the strength of the African branch of the Hadley circulation, which is linked to a decrease in the strength of the subtropical jet stream, extending eastwards to Australia. For these and other dynamically linked variables, most of the change occurs in a few years centred on the late 1960s. Some examples of this are shown in Figure 7. The correlations are dominated by the late 1960s change, and suggest that the variations in the Sahel rainfall drive the change in the Hadley circulation, which in turn affects the transport in the subtropical jet stream centred on 30°S. Here the transports are from NCEP reanalysis, and the rainfall from UEA and Aust. Bureau of Met. raingauge data sets.

The southwest corner region of the Australian continent lies on the northern flank of the main Southern Hemisphere storm track. A southward movement of the main storm track in the late 1960s of approximately 0.5° latitude, as identified by the latitude of the main storm track at

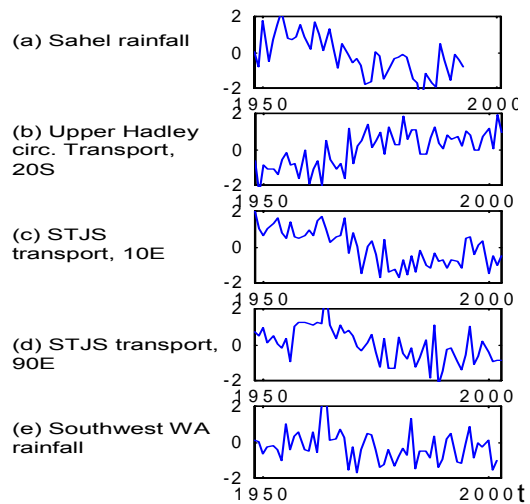


**Figure 7.** Time series of some key variables for JJA, normalized with their standard deviation. (a) Rainfall from the African Sahel (from M. Hulme, UEA); (b) mass transport in the upper branch of the Hadley circulation at 20°S, integrated over 20°W-15°E, 500-100 hPa; (c) mass transport in the subtropical jet stream at 10°E, integrated over 20°S-40°S, 500-100 hPa; (d) as for (c) but at 90°E; (e) Southwest Western Australia rainfall.

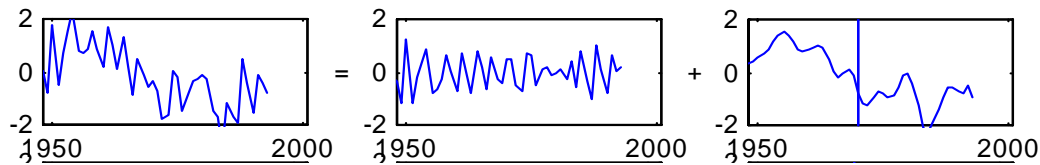


**Figure 8.** Rainfall for the African Sahel (here taken as 10°-20°N, 10°W-25°E) for JJA from M. Hulme UEA data set, decomposed using the empirical mode decomposition procedure of Huang et al. (1999), from 1948-1993. The first frame is the basic record as in Figure 7, the second is the interannual variation, and the third is the low frequency residual. The vertical dashed line denotes 1970.

90°E (Baines 2005), makes a plausible connection with the SWWA rainfall decrease. Hypothetically, a decrease in the southward heat flux from the Hadley circulation in the African sector implies a corresponding decrease in heat flux through mid-latitudes, and hence a less baroclinic state there. The simple criterion for two-layer instability (Phillips 1954) then implies that the storm track moves poleward, where the stabilizing  $\beta$ -effect that breaks the symmetry between the upper and lower baroclinic waves is weaker.

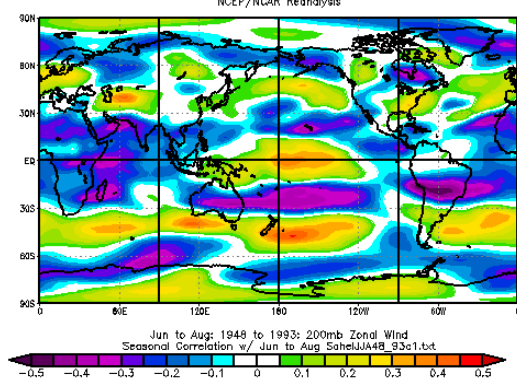


**Figure 9a.** A plot of the correlation coefficient of zonal wind for JJA at 200 hPa (from NCEP data) with the interannual component of the time series of Sahel JJA rainfall, shown in the central panel of Figure 8.

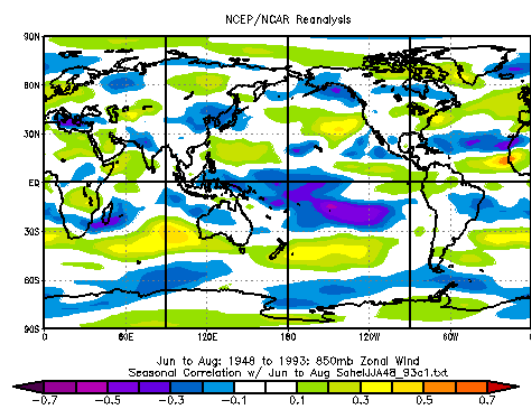


**Figure 9b.** As for Figure 9a but for 850 hPa.

The dependence of the mid-latitude circulation on tropical rainfall goes further than the 1960s change. Figure 8 shows a breakdown of the Sahel rainfall into interannual variations with zero local mean plus the low frequency residual, and the decrease in the late 1960s clearly resides in the latter. But if one correlates the interannual time series for this rainfall (central frame of Fig. 8) with the zonal winds in the upper and lower troposphere, one obtains correlation maps as shown in Figure 9. Zonal winds in the southern mid-latitudes and equatorial Pacific show substantial correlation with the Sahel rainfall, particularly in the upper troposphere.

The other major region that was affected by the 1960s shift was South America. Figure 10 shows the Brazilian rainfall for the region 0°-10°S, compared with rainfall from the Sahel. The decrease in the Sahel was accompanied by a remarkable increase in the rainfall in Brazil. Figures 11-13 take a closer look at the 1960s change in this region.

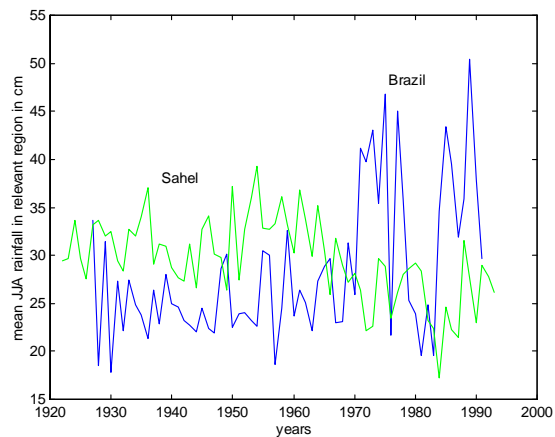


**Figure 10.** Rainfall over land in the region 0-10°S, east of 60°W, together with rainfall of the Sahel as defined above.

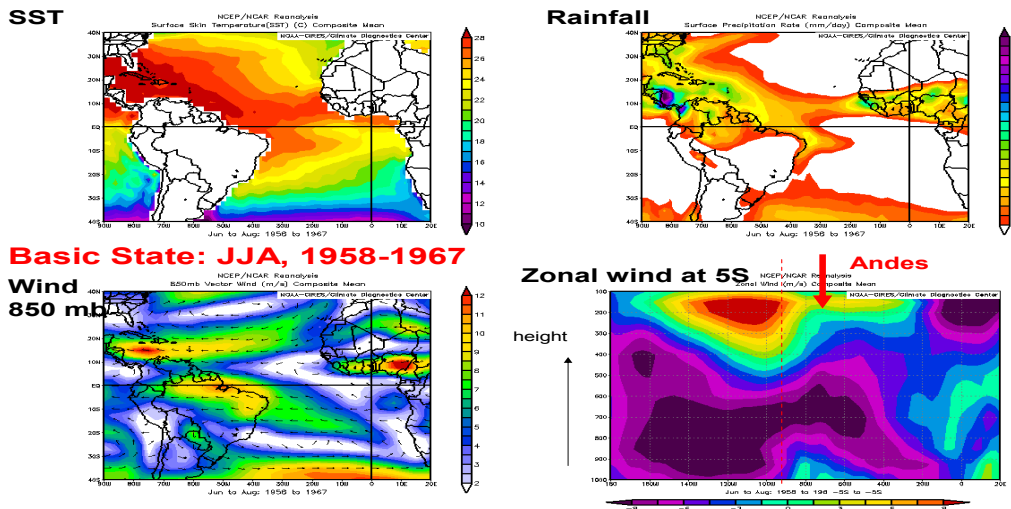


**Figure 11.** The basic state for JJA before the event, showing SST, rainfall, mean wind at 850 hPa and a vertical longitude-height section at 5°S.

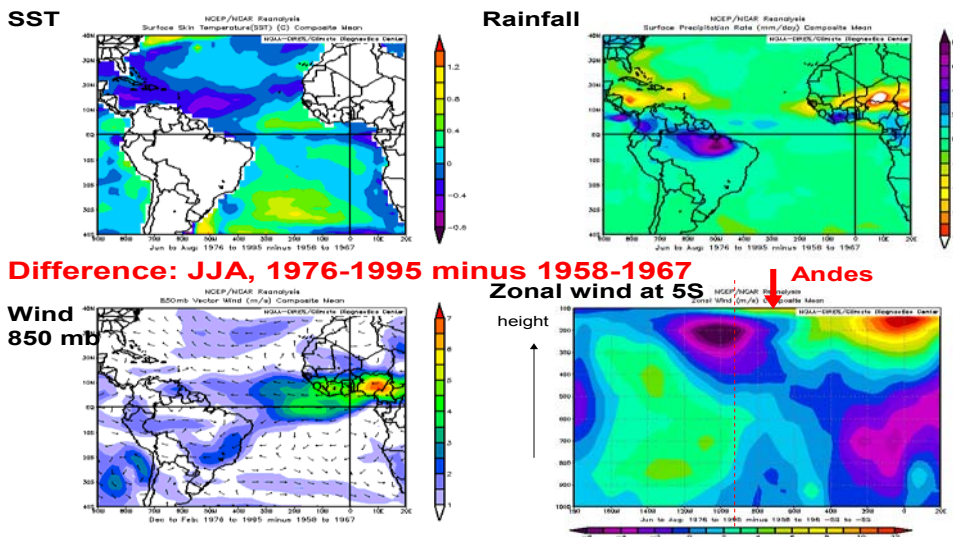


**Figure 12.** The same variables averaged over period 1976-1995, relative to 1958-1967, i.e. Figure 11.

**Mechanism for circulation, rainfall changes over South America – Africa:**

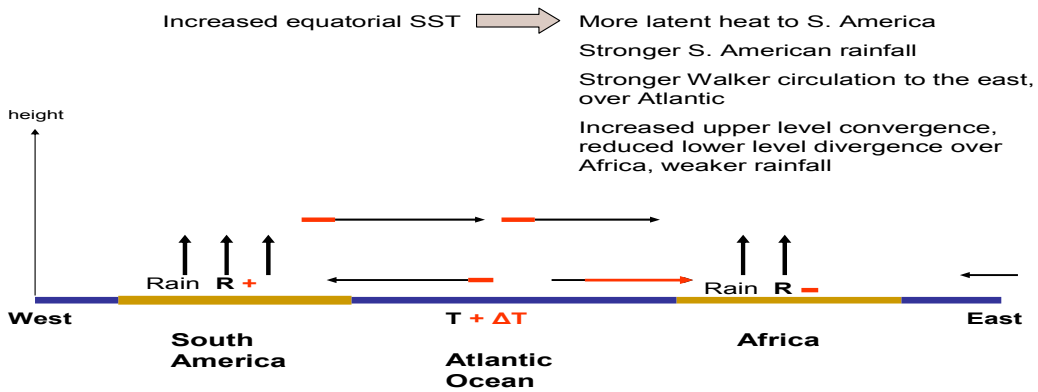


**Figure 13.** Schematic diagram of the dynamical connections between South American and African rainfall. Changes in the late 1960s are shown in red.

Figure 11 shows the mean state for the SST with warmer water north of the equator, and the rainfall regions in both Africa and Brazil being fed by the trade winds over long fetches. In the case of Africa, the wind direction changes after crossing the equator. Figure 12 shows that, after the 1960s shift, the equatorial SST increased, which is a contributor to the increased Brazilian rainfall. A substantial increase in this rainfall implies significant latent heat release which will produce an equatorial Kelvin wave response to the east, over the Atlantic and Africa, with easterly anomalies at low levels, westerlies at upper levels (Gill 1980). This low level anomaly will have the effect of reducing the inflow of moist air from the Atlantic into the African monsoon, and the Sahel region in particular. The westerly anomalies aloft may also be expected to contribute to reduced upper level divergence over Africa, with additional negative implications for African convection. This chain of events is illustrated schematically in Figure 13. The picture is qualitative, but the dynamical links between each stage in the process are well known.

This paper has said nothing about mechanisms for this climate shift; these are discussed in the manuscript by Baines & Folland cited above.

## REFERENCES

- Baines, P.G. 2005 Long-term variations in winter rainfall of Southwest Australia and the African monsoon. *Aust. Met. Mag.*, **54**, 91-102.
- Gill, A.E. 1980 Some simple solutions for heat-induced tropical circulation. *Quart. J. Roy. Met. Soc.* **106**, 447-462.
- Huang, N.E., Shen, Z., & Long, S. S. 1999 A new view of nonlinear water waves: the Hilbert Spectrum. *Ann. Rev. Fluid Mech.* **31**, 417-457.
- Kalnay, E. and Coauthors. 1996 The NCEP/NCAR Reanalysis 40-year Project. *Bull. Amer. Meteor. Soc.*, **77**, 437-471.
- Kistler, R. and 12 Coauthors. 2001 The NCER-NCAR 50-year Reanalysis: Monthly Means CD-ROM and Documentation. *Bull. Amer. Met. Soc.* **82**, 247-267.
- Lau, K.-M. and P.J. Sheu (1990) Teleconnections in global rainfall anomalies: seasonal to inter-decadal time scales. In *Teleconnections Linking Worldwide Climate Anomalies*, M.Glantz, W.Katz and N.Nicholls, Eds., Cambridge University Press, 227-256.
- Peixoto, J.P. & Oort, A.H. 1992 *Physics of Climate*, American Institute of Physics, New York, 520 pp.
- Phillips, N.A. 1954. Energy transformations and meridional circulations associated with simple baroclinic waves in a two-level, quasi-geostrophic model. *Tellus* **6**, 273-286.